Energy Engineering

Tech Science Press

DOI: 10.32604/ee.2022.020776

ARTICLE

Comparative Experimental Analysis on Coal Spontaneous Combustion

Haitao Wang[1,2], Yongli Liu[1,*], Bin Shen[1], Mengxuan Ren[1] and Qiyuan Shan[1]

[1]School of Safety Engineering, Heilongjiang University of Science and Technology, Harbin, 150028, China

[2]School of Resources Engineering, Heilongjiang University of Technology, Jixi, 158100, China

[*]Corresponding Author: Yongli Liu. Email: yongliliu1968@126.com

Received: 11 December 2021 Accepted: 28 February 2022

ABSTRACT

The goal of this study was to investigate coal quality features and their relationship to coal spontaneous combustion characteristics in multi-seam coal mines to better predict when coal spontaneous combustion is likely to occur. To that end, coal samples of various particle sizes were obtained from five coal seams (Nos. 6, 8, 9, 12 and 20) in the Shuangyashan City Xin'an Coal Mine. The samples were then respectively heated using a temperature programming system to observe and compare similarities and differences in the spontaneous combustion process of different particle sizes in response to rising temperature. The experimental results show, that in all five coal seams, the concentration of CO, C_2H_4, and C_2H_6 increased with a certain degree of regularity as a function of rising temperature. However, of these three gasses, only CO and C_2H_4 can be used as indicators to predict coal mine spontaneous combustion. The critical temperature for samples from all five coal seams ranged from 50–85°C, while the dry cracking temperature of coal seams 8 and 12 (80–100°C) were lower than those of 6, 9, and 20 (100–120°C). Furthermore, the production rate of CO, C_2H_4, and C_2H_6 is related to both coal particle size and temperature. The smaller the particle size, the faster the production rate; and the higher the temperature, the more gas that gets produced. All five coal seems are mainly composed of long flame coal. However, they differ in that the No. 12 coal seam contains weak cohesive coal; the No. 8 coal seam contains lean and gas coal; and the Nos. 6, 9, and 20 coal seams contain a certain amount of anthracite. During the programmed coal heating, the CO, C_2H_4, and C_2H_6 release trend for the coal seams was No. 12 > No. 8 > Nos. 6, 9, and 20. These results demonstrate that the presence of weak cohesive coal and anthracite highly influence the concentration of CO, C_2H_4, and C_2H_6 released during coal spontaneous combustion.

KEYWORDS

Coal quality analysis; spontaneous combustion; coal seam; index gas

1 Introduction

Coal is the most abundant energy source in China. By the end of 2020, there were 162.288 billion tons of coal in China's coal reserves [1], while China's 2020 coal production of 3.9 billion tons increased by 1.4% compared with 2019 [2]. Because coal is the safest and most economical source of energy in China [3], its dominant position in the energy structure cannot be replaced in the short term. However, as coal production increased, coal mine fire accidents increased in parallel, and has resulted in a large number of economic losses and casualties. According to incomplete statistics, in recent years, the number of coal mine fire accidents and associated fatalities, have decreased since 2000 [4]; likely

in response to the Chinese government strengthening efforts to prevent and control coal mine fire accidents. Nevertheless, major fire accidents still occur from time to time. Using the National Mine Safety Bureau Accident Data Query System, it was determined that the primary root cause of coal mine fires is coal spontaneous combustion [5] (Fig. 1).

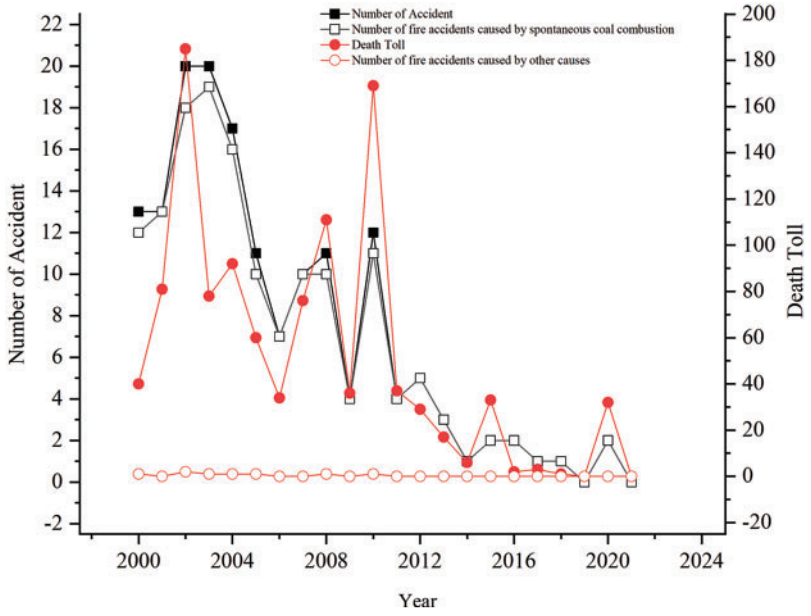

Figure 1: Coal mine fire accident statistics

Coal spontaneous combustion may occur in response to a combination of: coal crushing, coal accumulation and spontaneous combustion tendency, an oxygen concentration suitable for oxidation and adequate time for oxidation to develop, and heat storage conditions favoring exothermic oxidation. According to published research [6–13], the general consensus is that coal spontaneous combustion is a chain reaction that is generally divided into three stages: the low temperature oxidation stage, self-heating stage, and combustion stage (Fig. 2).

Numerous investigators have studied the spontaneous combustion characteristics of different coal types. Zhu et al. [14] used an adiabatic oxidation method to study and compare the dynamics associated with critical temperature and other parameters in coal of different grades. The relationship between the characteristic parameters and coal grade quality was numerically fitted, which provided a reference for prevention and control of coal spontaneous combustion. Tan et al. [15] investigated coal spontaneous combustion using temperature programmed testing and concluded that at the low temperature stage of coal spontaneous combustion, low metamorphic grade coal samples depict a higher oxygen consumption rate and heat release intensity than those of high metamorphic grade. Kim et al. [16] used oxidation experiments to study coal spontaneous combustion among coals of different rank, and proposed a low temperature reaction index to determine the spontaneous coal's combustion tendency. Dong et al. [17] carried out temperature-programmed oxidation experiments on various coal types. They determined that each coal type produced a different gas mixture and that gas production and temperature changed in an approximately exponential pattern. Furthermore, they also noted that: 1) as the coal becomes more metamorphosed, the sharp rise inflection point temperature in the gas production rate also increases; and 2) as the coal samples' oxidation capacity

decreases, the gas production decreases in parallel. Excluding the coal skeleton's complex structure, Clemens et al. [18] focused on the active coal structure and proposed a 10 reaction sequence coal oxidation adsorption reaction model. Mathews et al. [19] used modeling software to compare and analyze 133 kinds of active structures among brown, sub-bituminous, and smokeless coal to evaluate what governs changes to various active structures during coal spontaneous combustion. Wang et al. [20] established 13 elementary reactions that occur during the coal spontaneous combustion process, as well as their reaction order and secondary relationship. Their model has been successfully used for identifying coal spontaneous combustion tendency. Dai [21] studied structural changes to brown, gas, gas-fat, and smokeless coal samples under low temperature oxidation. Their results showed that differences in coal mine content and structure result in variations of low-temperature oxidation ability and spontaneous combustion tendency. Zhang et al. [22] examined parameter variations in primary and secondary oxidation of coal with different metamorphic degrees. Result showed that the lower the metamorphic degree, the higher the cross temperature range, and the greater the secondary oxidation spontaneous combustion parameters' change rate. Wen et al. [23] explored gas production during the oxidation process using long flame coal with different sulfur contents, and concluded that when considering coal of the same quality, higher sulfur content coal is more easily oxidized. Deng et al. [24,25] employed a temperature programmed device to study the influence of moisture on coal spontaneous combustion and determined the presence of an optimal critical value, which promotes coal spontaneous combustion before the critical value, and thus inhibits coal spontaneous combustion. Li et al. [26] conducted an adiabatic oxidation experiment to determine the mechanism by which ash content affects coal spontaneous combustion. They determined that a greater ash content results in a smaller temperature rise rate for low temperature oxidation stage coal samples, higher temperature rise acceleration point temperature, slower spontaneous oxidation process, weaker spontaneous combustion tendency, and more difficulty promoting coal spontaneous combustion.

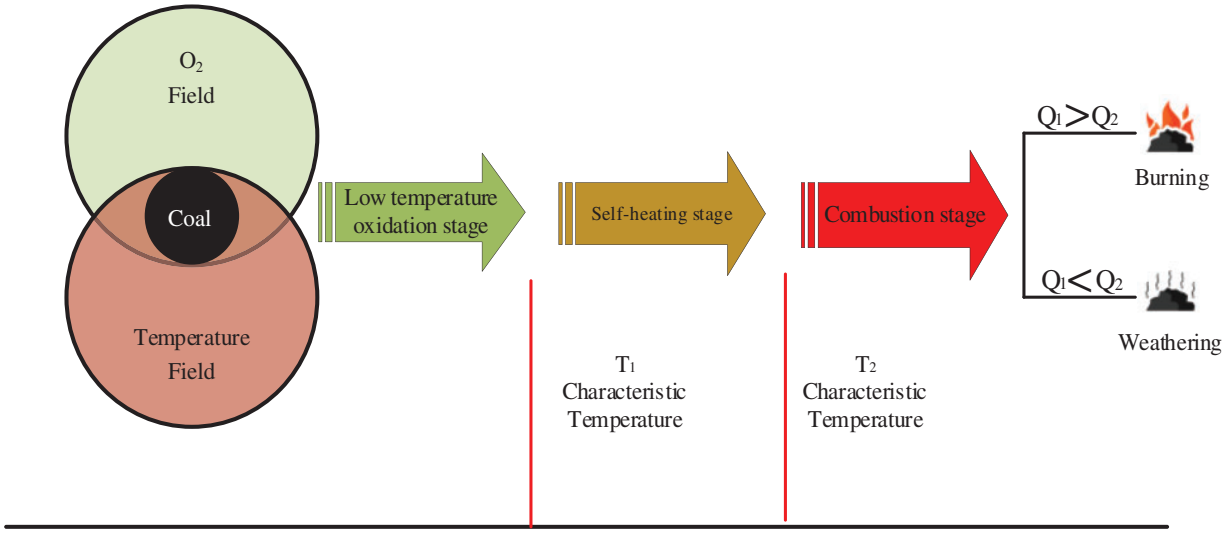

Figure 2: Coal spontaneous combustion process

China has a variety of multi-seam coal mines. Because the coal quality within each coal seam of a given mine differs, the corresponding coal spontaneous combustion characteristics differ as well. While the above mentioned studies explored coal spontaneous combustion characteristics among different types of coal, few studies have been conducted to evaluate coal spontaneous combustion characteristics of different coal types mixed in the same mine. To fill this gap, in this work, programmed heating equipment was used to conduct experiments on samples from five coal seams in the Shuangyashan Dongrong No. 2 Coal Mine. The goal was to analyze similarities and differences in the coal spontaneous combustion index gases and other parameters, to provide important reference for coal mine fire prediction in these environments.

2 Coal Spontaneous Combustion Theoretical Model

Below is an analysis and summary of the macro-physical model and micro-mathematical model associated with the coal temperature programmed experimental process, according to numerous domestic and internationally published literature [27–30]. These models improve the experimental principle macroscopically and explain the experimental mechanism microscopically. To begin, any point in the coal spontaneous combustion reaction vessel cylinder is selected for mathematical modeling. According to the heat balance principle (Eq. (1)):

$$\rho C_{\text{Coal}} \frac{\partial T}{\partial t} = QA^{\frac{-E}{RT}} + \lambda \frac{\partial^2 T}{\partial r^2} - H_{Water} \frac{dC_{Water}}{dt} + \rho_{Air} C_{Air} v_{Air} \frac{\partial T}{\partial \chi} \tag{1}$$

where:

C_{Coal}, C_{Water}, and C_{Air} are the specific heat capacities of coal, water, and air, respectively, J/(kg·°C);

Q is the heat generated by unit mass coal under standard conditions, J/kg;

ρ is density, kg/m^3;

v_{Air} is the gas flow rate in the coal samples;

A is the previous factor;

R is the gas constant—8.314 J/(K·mol);

T is temperature, °C;

E is activation energy, J/mol;

r is the inner diameter of the reactor, mm;

χ is the distance from bottom of the coal sample to its center, mm;

H_{Water} is the dry and wet heat, J/(m^3·s);

$\frac{dC_{Water}}{dt}$ is the dry and wet rate, 1/s;

λ is the heat conduction coefficient;

$\rho C_{\text{Coal}} \frac{\partial T}{\partial t}$ is the enthalpy change rate of the coal sample unit mass;

$Q\rho A^{\frac{-E}{RT}}$ is the coal oxidation heat production rate;

$\lambda \frac{\partial^2 T}{\partial r^2}$ is the heat conduction for the coal sample unit;

$H_{Water} \frac{dC_{Water}}{dt}$ is the enthalpy change rate for water evaporation; and

$\rho_{Air} C_{Air} v_{Air} \frac{\partial T}{\partial \chi}$ is the convection heat exchange between the gas unit and coal sample.

Triple integration of x, y, and z axes were performed for Eq. (1), and the real-time thermal function was obtained. Eq. (2) represents how coal in the reactor changes with time and temperature:

$$\left[\iiint \rho C_{Coal} dxdydz\right]\frac{\partial T}{\partial t} = \left[\iiint Q\rho dxdydz\right]A^{\frac{-E}{RT}} + \left[\iiint \lambda dxdydz\right]\frac{\partial^2 T}{\partial r^2} - \left[\iiint H_{Water} dxdydz\right]\frac{dC_{Water}}{dt} + \left[\iiint \rho_{Air} C_{Air} v_{Air} dxdydz\right]\frac{\partial T}{\partial \chi} \quad (2)$$

Eq. (3) was obtained by integrating Eq. (2):

$$m_{\text{Coal}} C_{\text{Coal}} \frac{\partial T}{\partial t} = Q m_{\text{Coal}} \text{A}^{\frac{-E}{RT}} + \lambda m_{\text{Coal}} \frac{\partial^2 T}{\partial r^2} - H_{Water} m_{\text{Coal}} \frac{\text{d}C_{Water}}{dt} + m_{Air} C_{Air} v_{Air} \frac{\partial T}{\partial t} \quad (3)$$

Eq. (3) was then transformed to obtain Eq. (4), which represents the heat of gas generated by coal spontaneous combustion:

$$m_{\text{Air}} C_{\text{Air}} v_{\text{Air}} \frac{\partial T}{\partial t} = m_{Coal} C_{Coal} \frac{\partial T}{\partial t} - Q m_{Coal} \text{A}^{\frac{-E}{RT}} - \lambda m_{Coal} \frac{\partial^2 T}{\partial r^2} + H_{Water} m_{Coal} \frac{\text{d}C_{Water}}{dt} \quad (4)$$

Eq. (4) is the energy conservation formula of the reactor. Because the mass of the generated gas is proportional to the heat, the generated gas heat target cannot be detected by determining the amount of generated gas. The macro physical model is shown in Fig. 3.

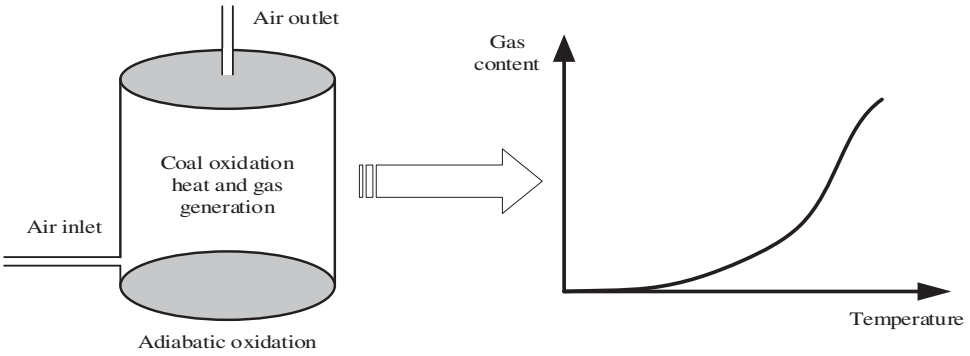

Figure 3: Macro physical model

3 Experimental Process

3.1 Determination of Coal Seam Coal Quality

Coal samples were collected from five coal seams in the Xin'an Coal Mine, in accordance with the national standard—GB/T 482-2008 (Sampling of coal seams). The industrial analysis coal experiment was carried out according to the national standard—GB/T 30732-2014 (Proximate analysis of coal-instrumental method), and the sulfur and phosphorous coal concentrations were determined according to the national standard—GB/T 214-2007 (Determination of total sulfur in coal). The coal's bond index was determined according to the national standard—GB/T 5447-1997 (Determination of caking index of bituminous coal). Finally, using the results from the above determinations, the type of coal was determined according to the national standard—GB/T 5751-2009 (Chinese classification of coals). The specific results from the coal determination analysis are shown in Table 1.

Table 1: Coal quality characteristics

Coal seam	Types of coal	Mad (%)	Ad (%)	Vdaf (%)	Std (%)	Pd (%)	Y (mm)	G
No. 6	Long-flame coal Lean coal Smokeless coal	6.15	11.02	29.19	0.12–0.33	0.039–0.043	0	2–6
No. 8	Long-flame coal Lean coal Gas coal	5.72	12.29	38.49	0.11–0.36	0.04–0.14	0	3–6
No. 9	Long-flame coal Smokeless coal	6.14	13.33	23.45	0.14–0.35	0.01–0.05	0	4–5
No. 12	Long-flame coal Weakly caking coal	5.5	16.15	41.79	0.20–0.35	0.01–0.001	0–6.5	4–35
No. 20	Long-flame coal Smokeless coal	7.1	18.58	21.69	0.30–0.45	0–0.008	0	4–5

Notes: *M = moisture; A = ash; V = volatiles; S = sulfur; P = phosphorus; Y = gelatine layer thickness; and G = adhesive index.

As shown in Table 1, there is little difference in the moisture, ash, sulfur, and phosphorus content among the selected coal samples and all four characteristics exhibit low values. In contrast, the volatiles show significant variation, and may be an important factor affecting the spontaneous combustion characteristics of coal. The coal samples are mainly composed of long bituminous coal. Samples from coal seams Nos. 6, 9, and 20 also contain anthracite, while those from No. 12 contain unique weak cohesive coal. The presence of weak cohesive coal leads to a higher coal bond index relative to other coal seams, which may be another important influence on the spontaneous combustion characteristics of coal.

3.2 Temperature Programmed Experimental Device

As shown in Fig. 4, the experimental system is divided into three parts: gas path, temperature control box, and gas sample collection and analysis.

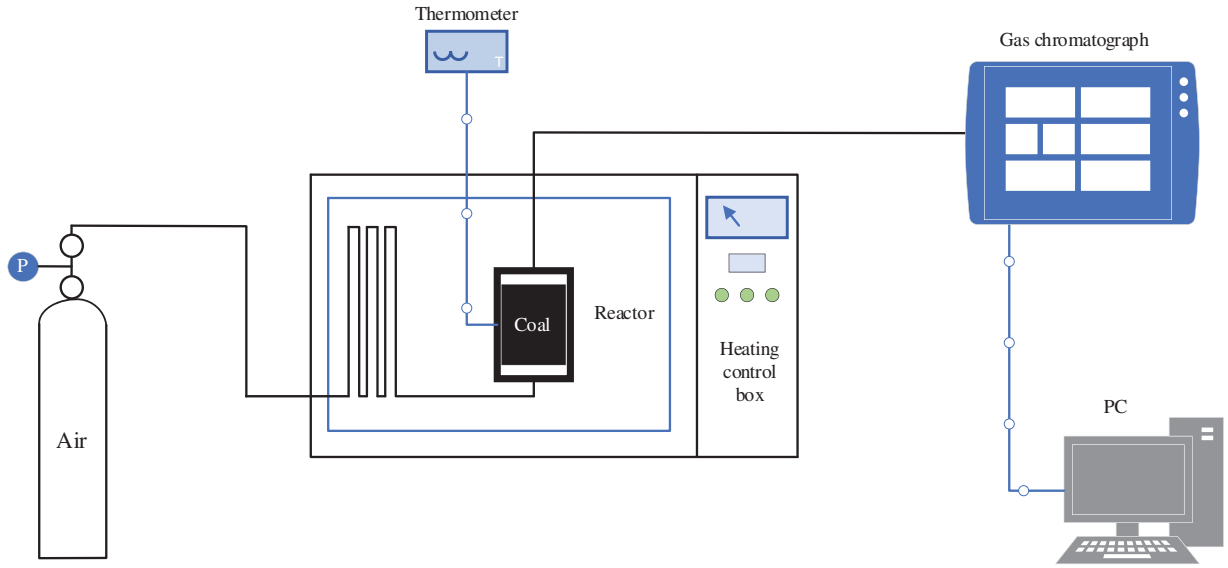

Figure 4: Temperature programmed experimental device

The air storage cylinder provided gas, via the flow control valve, that had been preheated in the temperature control box. This gas then flowed into the reactor, where it reacted with the coal. Subsequently, the gas discharged from the coal sample in the reactor was collected with a needle tube, then sent through an exhaust pipe (1 m long and 3 mm in diameter) to the gas chromatograph, where the gas composition was analyzed.

In order to reflect the coal samples' dynamic continuous oxygen consumption process and gas composition change under similar conditions to those in the actual mine, the coal spontaneous combustion test bench in Xi'an University of Science and Technology [31–33] was set using the following parameters: optimum reactor area = 70 cm^2, air supply = 120 ml/min, and the heating rate = 0.3 °C/min.

3.2.1 Experimental Process

A total of 25 kg of coal was collected from each coal seam. Next, the five coal samples were assembled based on particle size as follows: <0.9, 0.9–3, 3–5, 5–7, and 7–10 mm, respectively. Subsequently, 200 g of each particle size was mixed together to create a 1 kg, mixed particle size coal sample. Finally, the six prepared coal samples from each of the five coal seams, i.e., a total of 30 samples, were individually subjected to the programmed heating experiment.

A 1 kg coal sample was loaded into a 22 cm long, 10 cm diameter reactor. A net was used to hold the coal sample to make the ventilation uniform. The reactor was then placed in a temperature programmed box, such that ~2 cm of free space was at the upper and lower ends of the reactor. While the air heated according to the preprogrammed heating schedule, the gas produced from coal combustion was collected at different, predetermined temperatures. After the heating program completed its course, heating was terminated, and the furnace door was opened to enable natural convection cooling. Finally, the composition and concentration of the gas collected at the different temperatures were analyzed. Specific experimental parameters are listed in Table 2.

Table 2: Experimental parameters

Coal samples	Particle sizes (mm)	Average particle size (mm)	Height (cm)	Weight (g)	Volume (cm^3)	Volumetric weight (g/cm^3)	Porosity (%)	Air flow rate (ml/min)	Rate of temperature increase (°C/min)
No. 6	<0.9	0.45	15.70	1000	1232.45	0.81	0.44	120	0.3
	0.9–3	1.95	16.30	1000	1279.55	0.78	0.44		
	3–5	4.00	16.40	1000	1287.40	0.78	0.45		
	5–7	6.00	16.60	1000	1303.10	0.77	0.45		
	7–10	8.50	17.00	1000	1334.50	0.75	0.46		
	Mixed coal samples	4.18	15.60	1000	1224.60	0.82	0.42		
No. 8	<0.9	0.45	15.70	1000	1232.45	0.81	0.44		
	0.9–3	1.95	16.30	1000	1279.55	0.78	0.44		
	3–5	4.00	16.40	1000	1287.40	0.78	0.45		
	5–7	6.00	16.60	1000	1303.10	0.77	0.45		
	7–10	8.50	17.00	1000	1334.50	0.75	0.46		
	Mixed coal samples	4.18	15.60	1000	1224.60	0.82	0.42		
No. 9	<0.9	0.45	15.70	1000	1232.45	0.81	0.44		
	0.9–3	1.95	16.30	1000	1279.55	0.78	0.44		
	3–5	4.00	16.40	1000	1287.40	0.78	0.45		
	5–7	6.00	16.60	1000	1303.10	0.77	0.45		
	7–10	8.50	17.00	1000	1334.50	0.75	0.46		
	Mixed coal samples	4.18	15.60	1000	1224.60	0.82	0.42		
No. 12	<0.9	0.45	15.70	1000	1232.45	0.81	0.44		
	0.9–3	1.95	16.30	1000	1279.55	0.78	0.44		
	3–5	4.00	16.40	1000	1287.40	0.78	0.45		
	5–7	6.00	16.60	1000	1303.10	0.77	0.45		
	7–10	8.50	17.00	1000	1334.50	0.75	0.46		
	Mixed coal samples	4.18	15.60	1000	1224.60	0.82	0.42		
No. 20	<0.9	0.45	15.70	1000	1232.45	0.81	0.44		
	0.9–3	1.95	16.30	1000	1279.55	0.78	0.44		
	3–5	4.00	16.40	1000	1287.40	0.78	0.45		
	5–7	6.00	16.60	1000	1303.10	0.77	0.45		
	7–10	8.50	17.00	1000	1334.50	0.75	0.46		
	Mixed coal samples	4.18	15.60	1000	1224.60	0.82	0.42		

3.2.2 Results and Discussion

Carbon monoxide (CO) production analysis

Programmed temperature experiments were conducted to determine the relationship between CO release and temperature. Results for the five samples with different particle sizes (Figs. 5a–5e) from each coal seam and one mixed particle sample (Fig. 5f) from each coal seam are shown below.

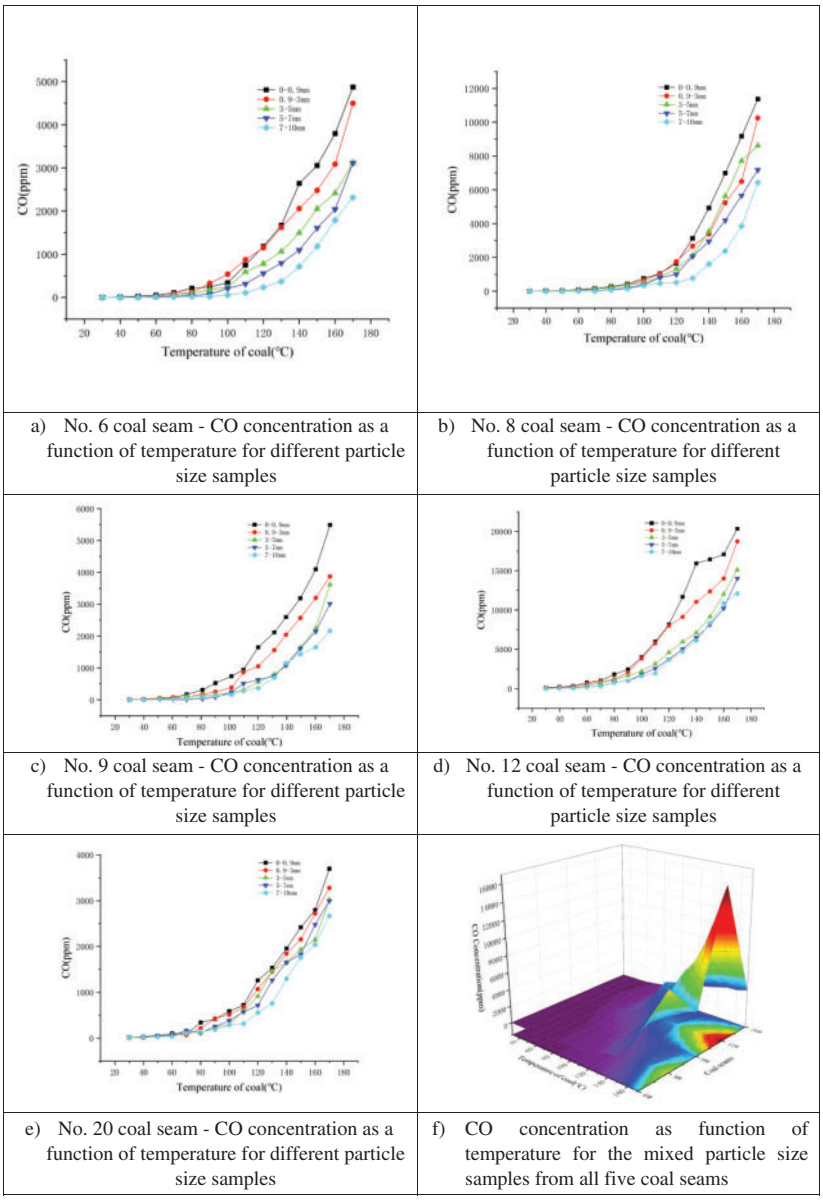

a) No. 6 coal seam - CO concentration as a function of temperature for different particle size samples

b) No. 8 coal seam - CO concentration as a function of temperature for different particle size samples

c) No. 9 coal seam - CO concentration as a function of temperature for different particle size samples

d) No. 12 coal seam - CO concentration as a function of temperature for different particle size samples

e) No. 20 coal seam - CO concentration as a function of temperature for different particle size samples

f) CO concentration as function of temperature for the mixed particle size samples from all five coal seams

Figure 5: Relationship between CO concentration and temperature for different particle size samples from coal seam a) No. 6, b) No. 8, c) No. 9, d) No. 12, and e) No. 20; and f) Mixed particle size samples for all five coal seams

As shown in Figs. 5a–5e, no CO gas was generated from 30–50°C, which indicates that the original coal sample did not contain CO. From 50–80°C, the relationship between CO concentration and particle size is not yet evident. However, at temperatures >80°C, the relationship between CO concentration and particle size became more apparent. The results indicate that the smaller the particle size, the larger the percentage of coal sample surface area that comes in contact with atmospheric oxygen, and the greater the oxygen consumption. This results in a more intense incomplete oxidation reaction between the coal and oxygen, which in turn generates more CO at a faster rate. As such, CO gas is a suitable coal seam spontaneous combustion index gas and can be used for monitoring

spontaneous combustion potential. Fig. 5f, which depicts the results from the mixed particle size samples, demonstrates that the largest quantity of CO was released by the sample from coal seam No. 12 (16270 ppm) and was followed by the sample from No. 8 (7772 ppm), while the samples from coal seams Nos. 6, 9, and 20 exhibited CO concentrations from 3000–4600 ppm.

C_2H_4 production analysis

Programmed temperature experiments were conducted to determine the relationship between C_2H_4 release and temperature. Results for the five samples with different particle sizes (Figs. 6a–6e) from each coal seam and one mixed particle sample (Fig. 6f) from each coal seam are shown below.

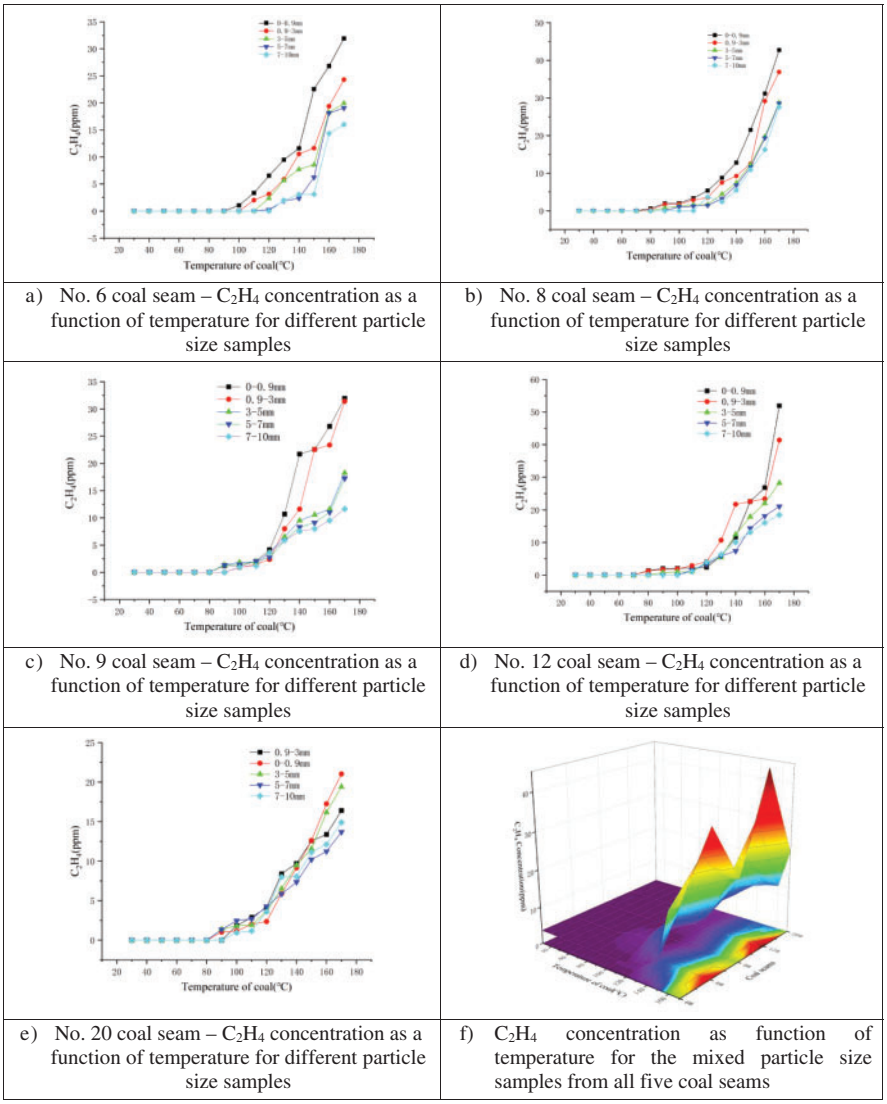

a) No. 6 coal seam – C_2H_4 concentration as a function of temperature for different particle size samples

b) No. 8 coal seam – C_2H_4 concentration as a function of temperature for different particle size samples

c) No. 9 coal seam – C_2H_4 concentration as a function of temperature for different particle size samples

d) No. 12 coal seam – C_2H_4 concentration as a function of temperature for different particle size samples

e) No. 20 coal seam – C_2H_4 concentration as a function of temperature for different particle size samples

f) C_2H_4 concentration as function of temperature for the mixed particle size samples from all five coal seams

Figure 6: Relationship between C_2H_4 concentration and temperature for different particle size samples from coal seam a) No. 6, b) No. 8, c) No. 9, d) No. 12, and e) No. 20; and f) Mixed particle size samples for all five coal seams

As shown in Figs. 6a–6e, C_2H_4 production sharply increased after the temperature reached 120°C. As with CO, the original coal sample did not contain C_2H_4; the C_2H_4 was generated due to high-temperature pyrolysis of the coal. In addition, the smaller the sample particle size, the more gas that gets produced; and the higher the temperature, the faster the gas production rate. As such, C_2H_4 gas is a suitable coal seam spontaneous combustion index gas and can be used for monitoring spontaneous combustion potential. Fig. 6f, which depicts the results from the mixed particle size samples, demonstrates that the largest quantity of C_2H_4 was released by the sample from coal seam No. 12 (52 ppm) and was followed by the sample from No. 8 (42 ppm), while the samples from coal seams Nos. 6, 9, and 20 exhibited C_2H_4 concentrations from 20–30 ppm.

C_2H_6 production analysis

The C_2H_6 variation by particle size in the five coal seams during the programmed temperature rise was analyzed using the superposition method. Results for the five samples with different particle sizes (Figs. 7a–7e) from each coal seam and one mixed particle sample (Fig. 7f) from each coal seam are shown below.

As shown in Fig. 7, C_2H_6 was observed at ~30°C, indicating that the original coal sample contained C_2H_6. Moreover, as the temperature increased, adsorbed C_2H_6 in coal sample was gradually released. Because C_2H_6 production occurs over the full temperature range, C_2H_6 is not useful for predicting coal spontaneous combustion and therefore is not a suitable indicator gas. Fig. 7f, which depicts the results from the mixed particle size samples, demonstrates that the largest quantity of C_2H_6 was released by the sample from coal seam No. 12 (2451 ppm) and was followed by the sample from No. 8 (2018 ppm), while the samples from coal seams Nos. 6, 9, and 20 exhibited C_2H_4 concentrations from 1000–1200 ppm.

Oxygen consumption and CO productionr rate of mixed coal samples

The mixed coal samples' variation in oxygen is mainly related to air convection, molecular diffusion, turbulent diffusion, and oxygen consumption by coal-oxygen interaction. Therefore, the convection-diffusion equation for oxygen concentration distribution is:

$$\frac{\partial C}{\partial t} = div(D \cdot \nabla(C)) - div(\frac{Q}{S}C) + V_{O_2}(T) \tag{5}$$

where: D is the oxygen diffusion coefficient in broken coal;

Q is the air supply, cm^3;

S is the furnace air supply area, cm^2;

C is oxygen concentration; and

$V_{O_2}(T)$ is oxygen consumption rate per unit of solid coal, $mol/(cm^3 \cdot s)$.

Under the experimental conditions, the air leakage intensity is small and mainly flows along the central axis. Therefore, it is reasonable to only consider the oxygen concentration distribution equation in the axial direction of coal body, which is mathematically expressed as:

$$\frac{\partial C}{\partial t} = \frac{\partial \left[D(\frac{\partial C}{\partial Z})\right]}{\partial Z} - \frac{\partial(\frac{Q}{S}C)}{\partial Z} + V_{O_2}(T) \tag{6}$$

where Z is the distance the gas flows through coal body, cm.

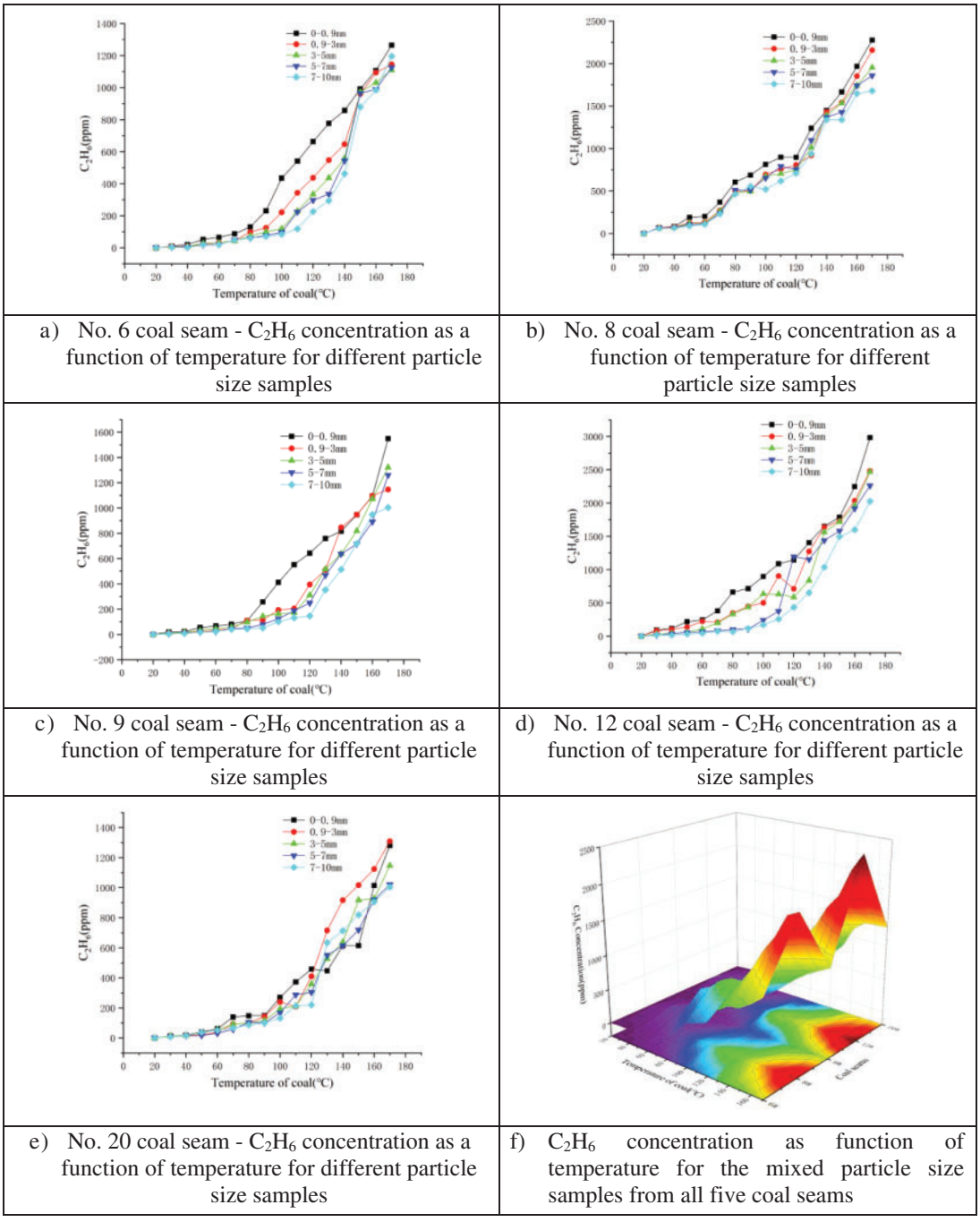

a) No. 6 coal seam - C_2H_6 concentration as a function of temperature for different particle size samples

b) No. 8 coal seam - C_2H_6 concentration as a function of temperature for different particle size samples

c) No. 9 coal seam - C_2H_6 concentration as a function of temperature for different particle size samples

d) No. 12 coal seam - C_2H_6 concentration as a function of temperature for different particle size samples

e) No. 20 coal seam - C_2H_6 concentration as a function of temperature for different particle size samples

f) C_2H_6 concentration as function of temperature for the mixed particle size samples from all five coal seams

Figure 7: Relationship between C_2H_6 concentration and temperature for different particle size samples from coal seam a) No. 6, b) No. 8, c) No. 9, d) No. 12, and e) No. 20; and f) Mixed particle size samples for all five coal seams

Since the oxygen consumption rate is proportional to the oxygen concentration, the oxygen consumption rate in fresh air is expressed as:

$$\frac{V_{O_2}^o(T)}{V_{O_2}(T)} = \frac{C_o}{C} \tag{7}$$

The oxygen consumption between any two points at the central axis is calculated using the following equation:

$$dC = -V_{O_2}^o(T) \times \frac{C}{C_o} \times \frac{S}{Q} dz \tag{8}$$

$V_{O_2}^0(T)$ and C_o are constant when the temperature is constant. Integrating both sides of Eq. (8) produces the following equation:

$$V_{O_2}^o(T) = \frac{Q \cdot C_o}{S \cdot (Z_{i+1} - Z_i)} \cdot \ln \frac{C_i}{C_{i+1}} \tag{9}$$

In the experimental system, because coal consumes oxygen, the oxygen concentration decreased and the CO concentration increased along the wind direction. The coal's CO production rate at a certain point in the reactor is proportional to the oxygen consumption rate, thus:

$$\frac{V_{CO}(T)}{V_{CO}^o(T)} = \frac{V_{O_2}(T)}{V_{O_2}^o(T)} = \frac{C}{C_o} \tag{10}$$

where: $V_{CO}(T)$ is the CO production rate, mol/(cm^3. s); and $V_{CO}^0(T)$ is the CO production rate at standard oxygen concentration, mol/(cm^3·s)

As such, the CO concentration at any point in the reactor can be calculated by combining Eqs. (9) and (10) as follows:

$$C_{i+1} = C_i \cdot e^{-\frac{V_{CO}^o(T) \cdot S}{Q \cdot C_0} \cdot (Z_{i+1} - Z_i)} \tag{11}$$

where: C_i is the oxygen concentration at a known point;

C_{i+1} is the oxygen concentration at the latter point;

Z_i is the distance from a known point to the entrance; and

Z_{i+1} is the distance from the latter point to the entrance.

Eq. (8) is then substituted into Eq. (11) and the CO production rate at standard oxygen concentration is obtained via integration, as shown in Eq. (12):

$$\begin{aligned} C_{o_2}^{i+1} - C_{o_2}^i &= \frac{S \cdot n \cdot V_{co}^0(T)}{Q \cdot C_0} \int_{z_1}^{z_2} C_1 \cdot e^{-\frac{V_0(T) \cdot S}{Q \cdot C_0} \cdot (Z_{i+1} - Z_i)} dz \\ V_{co}^o(T) &= \frac{V_O(T) \cdot (C_o^{i+1} - C_o^i)}{C_O \cdot [1 - e^{-\frac{V_0(T) \cdot S \cdot (z_2 - z_1)}{Q \cdot C_O}}]} \end{aligned} \tag{12}$$

Fig. 8 is based on Eqs. (9), (12), and the experimental data, and shows the relationship between temperature and the oxygen consumption rate (Fig. 8a) and CO production rate (Fig. 8b) of the mixed particle coal samples under fresh air conditions.

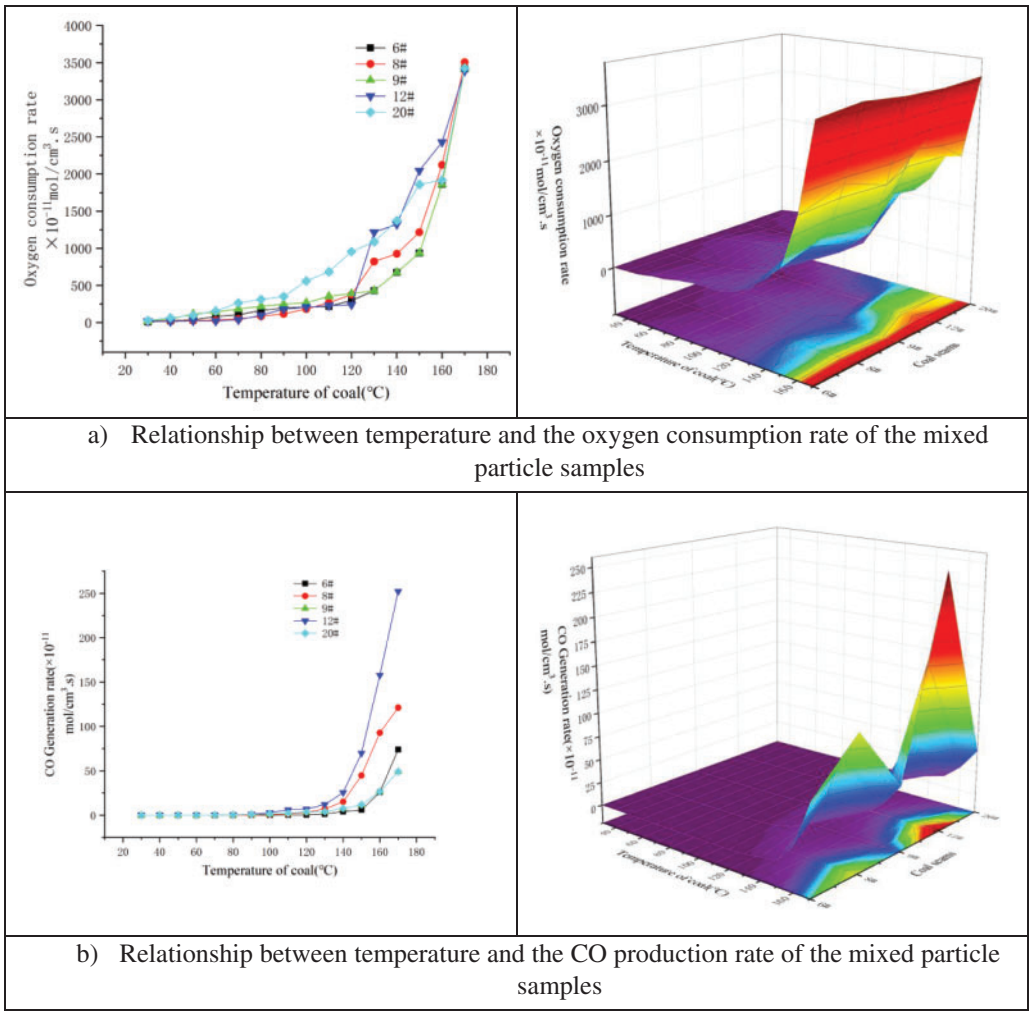

a) Relationship between temperature and the oxygen consumption rate of the mixed particle samples

b) Relationship between temperature and the CO production rate of the mixed particle samples

Figure 8: Relationship between temperature and a) oxygen consumption rate and b) CO production rate of mixed particle size coal samples

As shown in Fig. 8, the oxygen consumption rate of the coal samples from the Xin'an Coal Mine increased in response to increasing temperature. The mixed particle size coal samples had a large overall surface area and was therefore conducive to diffusing oxygen, which resulted in a relatively fast oxidation rate. The CO production rate increased significantly at 80–120°C, and then rapidly increased at temperatures >120°C. The CO production rate in the five sampled coal seams was as follows: No. 12 > No. 8 > Nos. 6, 9 and 20, with the latter three showing relatively low values.

4 Conclusion

In this work, programmed heating equipment was used to conduct experiments on samples of varying particle sizes from five coal seams in the Xin'an Coal Mine to observe and compare similarities and differences in the spontaneous combustion process in response to rising temperature. After analyzing the results, the following conclusions were drawn:

1) Based on the fact that the oxidation heat release intensity, CO production rate, oxygen consumption rate, and coal body heating rate all accelerate when the temperature exceeds 50–85°C, 50–85°C was determined as the critical temperature of the coal samples from the five coal seams in Xin'an Coal Mine. From 80–120°C, the oxygen consumption rate and CO gas production rate increased significantly and at temperatures >120°C, both increased sharply. Thus, it is inferred that the dry cracking temperature of coal seam Nos. 8 and 12 is 80–100°C, while that of Nos. 6, 9, 20 is 100–120°C. CO and C_2H_4 were not evident until the temperature exceed 80 and 110–120°C, respectively, demonstrating that both gasses were only produced at high temperature. In contrast, C_2H_6 appeared at about 30°C, indicating it was present in the original coal sample. Therefore, CO and C_2H_4 can be used as an index gas to predict coal spontaneous combustion, while C_2H_6 is not suitable for this purpose.
2) During thermal oxidation, the CO, C_2H_4, and C_2H_6 production rates and oxygen consumption rates differed based on the samples' particle size. In general, the CO, C_2H_4, and C_2H_6 concentration increased as the sample particle size decreased. While this trend is not very obvious in the low temperature stage, it is clearly evident in the high temperature stage. These results indicate that during the heating experiment, as the particle size decreased, the amount of surface area in contact with the oxygenated atmosphere gradually increased. As such, because coal samples easily oxidize, the coal-oxygen reaction played a progressively larger role, resulting in more CO, C_2H_4, and C_2H_6 being produced. In summary, the smaller the particle size, the greater the oxygen consumption, the more intense the incomplete oxidation reaction, and the more CO, C_2H_4, and C_2H_6 that gets produced.
3) Using a coal seam industry analysis, it was determined that all five coal seems depicted a low concentration of moisture, ash, sulfur, and phosphorus. Since large differences in volatiles and cohesiveness are the main factors affecting the coal's spontaneous combustion characteristics, these variables are thought to have little effect on the spontaneous combustion process. In contrast, coal type greatly influences the amount of gas produced by coal spontaneous combustion. Because the Nos. 8 and 12 coal seams do not contain anthracite, the coal is more easily oxidized, a lower amount of energy is required, and more CO, C_2H_4, and C_2H_6 is generated. Nos. 6, 9, and 20 coal seams all contain anthracite. Thus, the coal in these seams is not easily oxidized, and less CO, C_2H_4, and C_2H_6 was generated. These results verify that the presence or absence of anthracite highly influences the spontaneous combustion tendency of coal and that its spontaneous combustion tendency is lower than in other coal types.

Funding Statement: This work is grateful for the financial support from the Major Project of Engineering Science and Technology in Heilongjiang Province in 2020 (Grant No. 2020ZX04A01), and support from the Scientific Research Projects of Undergraduate Universities in Heilongjiang Province (Grant No. 2020-KYYWF-0534).

Conflicts of Interest: The authors declare that they have no conflicts of interest to report regarding the present study.

References

1. Ministry of Natural Resources of the People's Republic of China (2021). China mineral resources. http://www.mnr.gov.cn/sj/sjfw/.
2. China National Coal Association (2021). Annual report of coal industry development (2020). http://www.coalchina.org.cn/.

3. Wang, G. F., Ren, S. H., Pang, Y. H., Qu, S. J., Zheng, D. Z. (2021). Development achievements of China's coal industry during the 13th five-year plan period and future prospects. *Coal Science and Technology, 49(9),* 1–8. DOI 10.13199/j.cnki.cst.2021.09.001.
4. National Mine Safety Administration (2015–2022). National coal mine accident analysis report (2014–2021). https://www.chinamine-safety.gov.cn/.
5. National Mine Safety Administration (2022). Safety accident inquiry system of national mine safety administration. https://www.chinamine-safety.gov.cn/search/.
6. Qin, B. T., Zhong, X. X., Wang, D. M., Xin, H. H., Shi, Q. L. (2021). Research progess of coal spontaneous combustion process characteristics and prevention technology. *Coal Science and Technology, 49(1),* 66–99. DOI 10.13199/j.cnki.cst.2021.01.005.
7. Cudmore, J. F. (1988). Spontaneous combustion of coal and mine fires: By S. C. Banerjee (Editor), A. A. Balkema, Rotterdam, The Netherlands, 1985, xii + 168 pp.,Dfl. 68,25 (hardback). *International Journal of Coal Geology, 9(4),* 397–398. DOI org/10.1016/0166-5162(88)90034-1.
8. Banerjee, S. C., Chakravorty, R. N. (1967). Use of D.T.A. in the study of spontaneous combustion of coal. *Journal of Mines, Metals & Fuels, 15(1),* 1–5.
9. Muzyczuk, J. (1975). *Self-heating of coal during the oxidation process in an air stream in conditons approximately to adiathermal kommunicat*. No. 605–1974. Krakow, Poland, Amsterdam, The Nethorland: Glownego Instytutg Gornictwa, Kotowice, Poland.
10. Berkowitz, N. (1985). *The chemistry of coal. Science and technology*, vol. 7. Amsterdam, The Netherland: Elsevier.
11. Clarence, K. (1978). *Analytical methods for coal and coal products*. New York, San Francisco, London: Academic Press.
12. Gethner, J. S. (1985). Thermal and oxidation chemistry of coal at low temperatures. *Fuel, 64(10),* 1443–1446. DOI 10.1016/0016-2361(85)90348-5.
13. James, G. S. (1983). *The chemistry and technology of coal*. Berkeley, California: Chemical Industries, Heinz Heinemann, Inc.
14. Zhu, H. Q., Wang, H. Y., Song, Z. Y., He, C. Y. (2014). The relationship between oxidation kinetics characteristic parameters of coal adiabatic progress and metamorphic degree. *Journal of China Coal Society, 39(3),* 498–503. DOI 10.13225/j.cnki.jccs.2013.0409.
15. Tan, B., Hu, R. L., Li, K., Bao, T. S., Fan, W. B. (2013). Comparison analysis on spontaneous combustion limit parameters of bituminous coal with different metamorphic degree. *Coal Science and Technology, 41(5),* 63–67. DOI 10.13199/j.cst.2013.05.73.tanb.019.
16. Kim, J., Lee, Y., Ryu, C., Park, H. Y., Lim, H. (2015). Low-temperature reactivity of coals for evaluation of spontaneous combustion propensity. *Korean Journal of Chemical Engineering, 32(7),* 1297–1304. DOI 10.1007/s11814-014-0331-9.
17. Dong, X. W., Wang, F. S., Meng, Y. N. (2014). Study on the characteristics of gas products in heating and oxidation process of different coal. *Journal of Safety Science and Technology, 10(3),* 48–53. DOI 10.11731/j.issn.1673-193x.2014.03.008.
18. Clemens, A. H., Matheson, T. W., Rogers, D. E. (1991). Low temperature oxidation studies of dried New Zealand coals. *Fuel, 70(2),* 215–221. DOI 10.1016/0016-2361(91)90155-4.
19. Mathews, J. P., Chaffee, A. L. (2012). The molecular representations of coal—A review. *Fuel, 96,* 1–14. DOI 10.1016/j.fuel.2011.11.025.
20. Wang, D., Xin, H. H., Qi, X. Y., Dou, G. L., Zhong, X. X. (2014). Mechanism and relationships of elementary reactions in spontaneous combustion of coal the coal oxidation kinetics theory and application. *Journal of the China Coal Society, 39(8),* 1667–1674. DOI 10.13225/j.cnki.jccs.2014.9017.
21. Dai, G. L. (2011). Research on microcrystalline structure change regularity in the coal low temperature oxidation process. *Journal of China Coal Society, 36(2),* 322–325. DOI 10.13225/j.cnki.jccs.2011.02.018.

22. Zhang, X. H., Li, Q. W., Xiao, Y., Lu, J. H., Deng, J. (2016). Experiment study on the limit parameters of the forsaken coal spontaneous combustion in the re-oxidation process. *Journal of Safety and Environment, 16(4),* 101–106. DOI 10.13637/j.issn.1009-6094.2016.04.020.
23. Wen, H., Zhang, F. Y., Jin, Y. F., Liu, W. Y. (2011). Experiment research on effect of sulfur on characteristic parameters of coal. *Safety in Coal Mines, 42(10),* 5–7. DOI 10.13347/j.cnki.mkaq.2011.10.034.
24. Deng, J., Liu, W. Y., Zhai, X. W., Hu, W. (2011). Research on the effects of moisture on oxidation and spontaneous combustion properties of mengba coal mine. *Safety in Coal Mines, 42(11),* 15–19. DOI 10.13347/j.cnki.mkaq.2011.11.018.
25. Liu, W., Jin, Y., Deng, J., Zhao, R. (2013). Experimental study on influence of moisture on coal's characteristic temperature in Mengba Mine. *Mining Safety & Environmental Protection, 40(4),* 1–3+7.
26. Li, L., Chen, J. C., Jiang, D. Y., Zhu, T. X. (2017). Experimental study of the impact of ash on spontaneous combustion characteristics of coal. *Journal of Chongqing University, 40(4),* 85–92. DOI 10.11835/j.issn.1000-582X.2017.04.011.
27. Zhong, X. X., Li, L. D., Chen, Y. (2016). Changes in thermal kinetics characteristics during low-temperature oxidation of low-rank coals under lean-oxygen conditions. *Energy & Fuels, 31(1),* 239–248. DOI 10.1021/acs.energyfuels.6b02197.
28. Naktiyok, J., Bayrak, H., Özer, A. K., Gülaboğlu, M. Ş. (2017). Investigation of combustion kinetics of umutbaca-lignite by thermal analysis technique. *Journal of Thermal Analysis and Calorimetry, 129(1),* 1–9. DOI 10.1007/s10973-017-6149-z.
29. Chen, X. D. (1992). On the mathematical modeling of the transient process of spontaneous heating in a moist coal stockpile. *Combustion & Flame, 90(2),* 114–120. DOI 10.1016/0010-2180(92)90113-4.
30. Lu, W., Cao, Y. J. X., Huang, Z. A., Tien, J. C., Qin, B. T. (2017). Study on adiabatic oxidation characters of coal with applying a constant temperature difference to guide the oxidation of coal with temperature rising. *Energy & Fuels, 31(1),* 882–890. DOI 10.1021/acs.energyfuels.6b02247.
31. Liu, W. Y. (2019). *The thermal effect of coal oxidation spontaneous combustion and adiabatic spontaneous combustion period* (*Master Thesis*). Xi'an University of Science and Technology, China.
32. Fei, J. B. (2019). *Study on the determination theory of coal spontaneous combustion stage and classification warning method* (*Master Thesis*). Xi'an University of Science and Technology, China.
33. Gao, K. (2012). *Research on prediction method of coal spontaneous combustion based on support vector machine* (*Master Thesis*). Xi'an University of Science and Technology, China.